Journal of Coastal Research	SI 64	1911 - 1915	ICS2011 (Proceedings)	Poland	ISSN 0749-0208

Storm-Surge Inundation along a multibarred beach

A. Sancho-García†, B.G. Ruessink‡ and J.Guillén†

†Marine Geology Department, Marine Science Institute (ICM-CSIC), 08003 Barcelona, Spain. asancho@icm.csic.es

‡ Department of Physical Geography, Faculty of Geosciencies, Institute for Marine and Atmospheric Research, Utrecht University. P.O. Box 80.115, 3508 TC Utrecht, The Netherlands

ABSTRACT

Sancho-Garcia, A., Ruessink, B.G. and Guillén, J., 2011. Storm surge inundation along a multibarred beach. Journal of Coastal Research, SI 64 (Proceedings of the 11th International Coastal Symposium), 1911 – 1915. Szczecin, Poland, ISSN 0749-0208

Coastal inundation during storms is produced by the addition of the storm surge and the wave run-up, which depends on setup and swash, to the astronomical tide level. Here, we use video monitoring techniques to estimate the inundation at the beach of Noordwijk (The Netherlands) during the seven strongest storms in the period between 1998 and 2005. Inundation values ranged from 22 to 112 m, with considerable alongshore variation before the peak of each storm. In addition, we demonstrate that mean inundation values along the beach are well estimated using a simple parameter that includes the intertidal and the supratidal beach slope, deep-water wave height and wavelength and the surge level.

ADITIONAL INDEX WORDS: *video-imagery, beach morphology, inundation, storm surge*

INTRODUCTION

A considerable portion of the world's population lives in coastal areas and is exposed to hazards, such as coastal erosion and flooding, that are produced by sediment starvation, storms, tsunamis, sea level rise, etc (Ferreria *et. al*, 2006). The water level increases considerably during storms, due to the storm surge and the wave run-up which results from set-up and swash (Stockdon *et al.,* 2006). A storm surge is generated by extreme wind stress acting on shallow continental shelf seas and can lead to severe coastal inundation. A well-known example is the storm surge of 31 January-1 February 1953 that caused considerable damage and loss of live in the Netherlands and the United Kingdom (Wolf and Flather, 2005; Brown *et. al*, 2007).

Coastal inundation is an instantaneous process and quantitative measures of this phenomenon used to be scarce; however, video monitoring techniques nowadays provide frequent and accurate measurements of coastal inundation (Sancho-García *et al.*, 2008). The main aim of this study is to quantify the inundation produced during severe storms at a sandy multiple-bar microtidal beach (Noordwijk, The Netherlands) using video monitoring. Furthermore, we test a simple inundation parameter, comprising a run-up expression, the offshore wave conditions, the surge level and the beach foreshore slope, and demonstrate that inundation at this beach is governed primarily by the storm surge level.

FIELD SITE

Noordwijk is located on the central Dutch coast, oriented 28º from the North and facing the semi-enclosed North Sea (Figure 1). It is a sandy, wave-dominated coast with a beach and nearshore zone that consists of a single intertidal slip-face ridge and two subtidal bars. Occasionally, a second intertidal bar may form on a pre-existing bar during low-energy wave conditions (Quartel *et al.,* 2007). The waves, mainly incident from southwestern to northwestern directions, have an average offshore root-mean-square (rms) wave height of 0.7 m and a corresponding period of 6 s. The tide at Noordwijk is semi-diurnal and microtidal. The mean tidal range is 1.8 m and 1.4 m during spring and neap tide respectively.

METHODS

Storm events between 1999 and 2005 were selected using hourly records of offshore wave and water level collected at Meetpost Noordwijk (MPN in Figure 1) which is located 9.5 km offshore at 18-m water depth. Gaps in the wave data series were filled with data from Europlatform (EUR in Figure 1), located 21 km offshore in 30-m water depth. We selected storm events as periods of at least 30 hours during which the offshore root-mean square wave heights, Hrms, exceeded 2 m and the surge level (η_{surge}, defined as the difference between measured and astronomical water levels, η_{meas}- η_{pred}) was larger than 0.5 m. The threshold for the start and the end of each storm was a Hrms less than 1.5 m and a positive surge level. Here we focus on the seven largest storms (Table 1).

Beach inundation for each storm event was obtained hourly by means of an Argus video system (Holman and Stanley, 2007). This video system is mounted on the top of a hotel at a height of 62 m above mean sea level, and consists of five cameras that together view the coast over 6 km in the alongshore direction, and 1·5 km in the cross-shore direction. Images are in the visible range of light and the sampling is done every daylight hour during a ten-minute period (2 pictures per second). The 10-minute average time

Table 1: Characterization of storm events.

Event	Initial day	$Hrms_{mean}$ (m)	$Hrms_{max}$ (m)	Mean Tp (s)	Mean Direction (º)	η_{surge} (mean) (m)	η_{surge} (max) (m)	Duration (h)
1	27/10/1998	2.3	3.4	7.8	272 (W)	0.7	1.3	98
2	16/02/1999	2.4	3.5	8.3	310 (NW)	0.8	1.2	49
3	21/02/1999	2.2	3.2	8.0	305 (NW)	0.7	1.1	64
4	07/09/2001	2.1	2.7	7.8	326 (NW)	0.6	0.8	88
5	22/02/2002	2.4	3.2	8.0	294 (WNW)	0.7	1.2	45
6	05/10/2003	2.2	3.4	8.0	295 (WNW)	0.5	1.1	69
7	15/12/2005	2.7	3.3	8.6	333 (NNW)	0.7	1.2	69

Argus images were geometrically transformed to obtain a rectified plan view of the beach and the nearshore zone. The region of interest covered 900 m in the alongshore with the camera position in the left side and 300 m, in the cross-shore direction. The pixel size of the rectified images was 1 x 1 m.

The hourly waterline position was extracted from each plan view by the automated alongshore tracking of the intensity maxima across the waterline (Pape *et. al*, 2010). These high intensities are generated by the swash-induced foam. In total, our data set comprise 184 waterlines.

We define beach inundation as the distance between the observed instantaneous waterline and the theoretical waterline position induced by the astronomical tide only. Thus, in order to obtain the inundation, the theoretical position of the waterline related to the astronomical tide had to be estimated. The waterline was extracted from the overall images dataset during low-energy conditions (Hrms<0.7 m and a surge level ± 3 cm) and with an astronomical tide around ±5 cm of -1, -0.75, -0.5, -0.25, +0.25, +0.5, +0.75 and +1 m. A linear regression between the alongshore-averaged position of each waterline and the corresponding astronomical tide was computed for each year considering a constant beach slope. The slope of this linear regression was the intertidal beach slope (β_{int}) (Table 2). Finally, beach inundation was calculated as the distance between the waterline and the theoretical waterline position considering only the astronomical tide along shore-normal beach profiles defined every meter (Figure 2).

The hourly observed inundation at each profile was compared with an inundation parameter, I_p (1), which includes the beach slope (β), a run-up expression (adapted from Stockdon *et al.*, 2006), $\beta\cdot(H_oL_o)^{0.5}$, where Ho and Lo are the deep-water wave height and wavelength respectively, and the surge level (η_{surge}),

$$I_p = \left[\frac{\beta g \left(H_o g L_o \right)^{0.5} + \eta_{surge}}{\beta} \right] \quad (1)$$

The beach profile is represented as two lines with different slopes and so that two different beach slopes were defined in order to apply the inundation parameter, I_p: the intertidal beach slope, (β_{int}), calculated previously and the supratidal beach slope (β_{sup}) estimated from annual beach topographic surveys. The limit to consider and use the supratidal or intertidal beach slope was a water level of +0.9 m NAP (≈Dutch ordinance level, ≈ mean sea level) because it is the mean maximum water level of the waterlines considering only the astronomical tide.

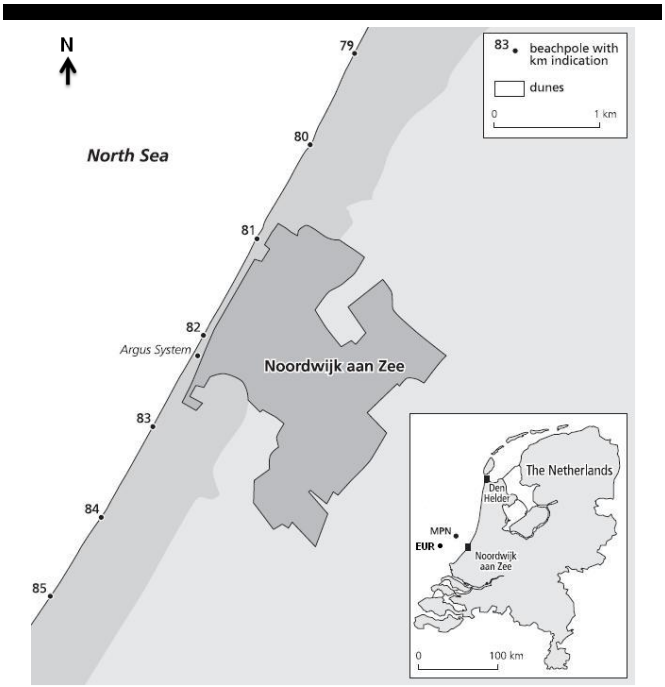

Figure 1. Study area with the hydrodynamic data collection: Meetpoint Noordwijk (MPN) and Europlatform (EUR), and with the position of the Argus station. Beach poles indicate distance in kilometres from a regional zero. Beach pole 82 corresponds to y=0.

Intertidal beach slope values were typically 1:60, characteristic of a dissipative beach, with little interannual variability (Table 2). The supratidal beach was steeper, typically 1:25 (Table 2).

RESULTS

The seven storms selected were characterized by wave directions from West to North-northwest, surge levels from 0.5 to 1.3 m and wave heights from 1.5 to 3.5 m. The inundation was smallest during events 1 and 4, and largest during events 3 and 6. Observed inundation values varied from 22 m to 112 m. In general, the inundation was alongshore non-uniform before the peak of each storm, except for event 3, and alongshore uniform during and after the peak of the storm.

For similar surge levels and wave heights, inundation values were lower during high tide than low tide. For instance, during

event 7 the alongshore-averaged inundation was 20 m and 103 m at high and low tide, respectively (Figure 3).

The correlation-coefficient squared R^2 between the alongshore-averaged observed inundation and the predicted inundation, $I_{p,}$ amounted to 0.77. The root-mean-square difference between observations and predictions (rmse) amounted to 11.70 m (Figure 4). In more detail, event 3 resulted in the highest correlation, R^2 = 0.91 (rmse = 8.84 m), and event 4 in the lowest, R^2 = 0.65 (rmse = 12.36) (Table 2).

Finally, the most drastic change in the correlation coefficient along the beach was observed in event 6, in which the R^2 decreased from 0.75 (rmse ≈ 12 m) to 0.45 (rmse ≈ 17 m) along a distance of 300 m.

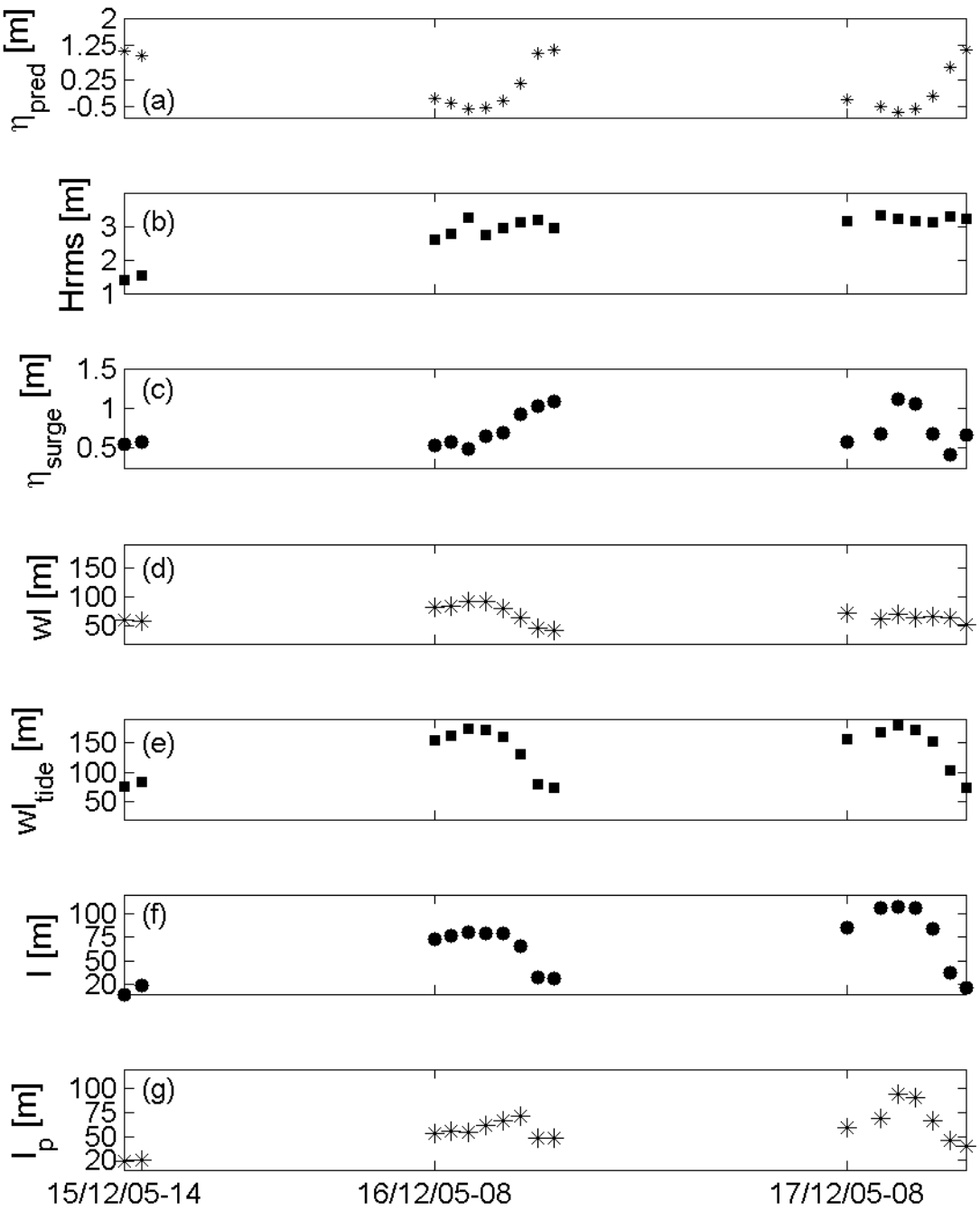

Figure 2. Hydrodynamic conditions and inundation at one profile (y = -400 m) for the Event 7. (a) Astronomical tide level; (b) Offshore root-mean-square wave height; (c) Surge level; (d) Cross-shore position of the waterline; (e) Theoretical cross-shore position considering only the astronomical tide; (f) Inundation; (g) Inundation parameter (Eq. 1). Note that cross-shore distance is positive going offshore, hence a decrease to 0 in (d) and (e) indicates that the waterline is located further landward.

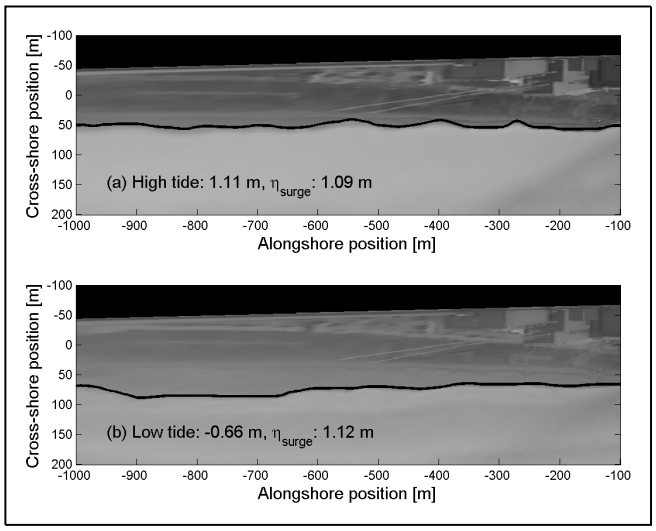

Figure 3. Inundation for event 7 at high tide (a) and at low tide (b). Positions are given in Argus coordinates.

DISCUSSION

In general, alongshore non-uniform inundation resulted from alongshore non-uniformity in the intertidal bars, present before the storm. As can be seen in Figure 5, the alongshore shapes of the intertidal bar existing some days before the beginning of event 1 and the waterlines before the peak of storm had the same alongshore variation. After event 1, both were uniform. Due to the long storm duration (>30h), large Hrms (≥2m) and large positive surge levels (≥0.5m), the intertidal bars are likely to be destroyed during each storm (Quartel *et al.*, 2007), causing the inundation to become more uniform alongshore. For this reason, events 2 and 3, which were two consecutives northwest storms separately by approximately three days only, differed in behavior. The time span between events 2 and 3 was too short for intertidal sandbars to form and hence the inundation during event 3 was for more uniform prior to its peak than during event 2.

Brown *et al.* (2007) suggested that the coastal inundation can be severe during storm surge events particularly when they coincide with a high tide and result in overtopping and breaching. However, overtopping and/or breaching did not occur during the studied storms. Accordingly to our results during high tide conditions, inundation was less than during low tide. An explanation would be that during these conditions the waterline is located in the supratidal zone of the beach where the slope is twice higher than the intertidal beach slope and therefore less inundation could be produced. The storms analyzed here are characterized by water levels less than +3 m NAP, not as extreme as during the 1953 storm. This storm was characterized by a significant wave height of 8 m and a large surge (4 m), produced by northern winds, which combined with a high spring tide produced particular high water levels and therefore catastrophic inundation (Wolf and Flather, 2005).

In order to evaluate the contribution of the wave run-up and the surge processes in the inundation at Noordwijk, both terms were independently correlated to the alongshore-averaged inundation. Considering only the surge level term the correlation was R^2 = 0.62 (rmse ≈ 14 m) whereas using only the run-up term the correlation decreased to R^2 = 0.31 (rmse ≈ 20 m). This suggests that events depended mainly on surge levels. Analyzing event by event, the correlation in almost all events was more or less equal (events 2, 3, 4, 5), worse for event 1 and 6 and even better for event 7 (R^2 = 0.79, rmse ≈ 15 m) when only the surge level was considered (Table 2). Event 7 is characterized by a wave direction of north-northwestern which is the direction from which the largest waves arrive (Wolf and Flather, 2006; Quera, 2010). At the North-Sea, winds from these directions produces large surge and therefore this will explain the better correlation when the inundation parameter only includes the surge level. On the other hand, event 4 was characterized by a constant northwest wave direction and wave heights and surge levels values approximately constant during the event, yet it produced the lowest correlation. The reason for this is not well understood.

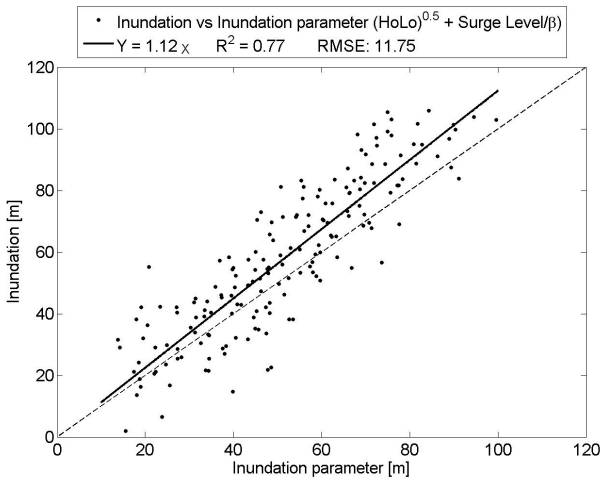

Figure 4. Inundation parameter versus alongshore-averaged observed inundation. Solid line represents the best fit to the data and dashed line is a 1:1 line.

CONCLUSIONS

A new methodology for calculating the inundation in a sandy multiple-bar microtidal beach using video observations has been developed and applied to Noordwijk beach in the Netherlands. The estimated inundation varied between 22 and 112 m, and was non-uniform in the alongshore prior to the peak of a storm because of alongshore variations in the intertidal sandbars. During the peak of the storm, most of the intertidal sandbars disappeared and the inundation then became more uniform in the alongshore. Our simple inundation parameter, $I_{p,}$ that includes a run-up expression and the surge level, estimated the observations reasonably well and indicated that the surge level was the main factor influencing the magnitude of the inundation. We believe that our inundation parameter can be used as a predictive tool to forecast inundation and be useful to highlight the critical situations that might result in severe dune erosion or infrastructural damage.

LITERATURE CITED

Brown, J.D., Spencer, T., and Moeller, I. 2007. Modelling storm surge flooding of an urban area with particular reference to modeling uncertainties: A case study of Canvey Island,

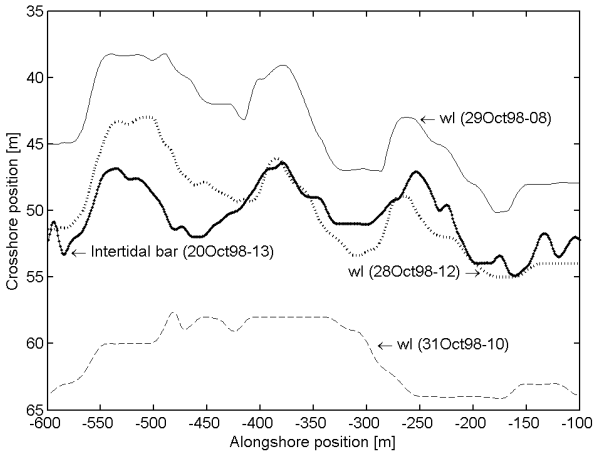

Figure 5. Waterlines and intertidal bar line during the event 1 (October, 1998). Cross-shore and alongshore position are given in Argus coordinates.

United Kingdom. *Water Resources Research*, 43, W06402, doi: 10.1029/2005WR004597.

Holman, R.A., and Stanley, J. 2007. The history and technical capabilities of Argus. *Coastal Engineering*, 54, 447–491.

Ferreira, O., García, T., Matias, A., Taborda, R., and Alveirinho Dias, J. 2006. An integrated method for the determination of set-back lines for coastal erosion hazards on sandy shores. *Continental Shore Research*, 26, 1030-1044.

Pape, L., Plant, N.G. and Ruessink, B.G. 2010. On cross-shore sandbar behavior and equilibrium states. *Journal of Geophysical Research - Earth Surface*, 115, F03008, doi:10.1029/2009JF001501.

Plant, N.G., Aarninkhof, S.G.J., Turner, I.L, and Kingston, K.S. 2007. The performance of waterline detection models applied to video imagery. *Journal of Coastal Reserach*, 23 (3), 658-670.

Quera, Q. 2010. Evaluation of the nourishments and the Dutch coast protection policy for the Noordwijk coast (The Netherlands). *Master thesis Utrecht University*, 79 pp.

Quartel, S., Kroon, A., and Ruessink, B.G.,. 2008. Seasonal accretion and erosion patterns of a microtidal sandy beach. *Marine Geology*, 250, 18-22.

Quartel, S., Ruessink, B.G. and Kroon, A. 2007. Daily to seasonal cross-shore behavior of quasi-persistent intertidal beach morphology. *Earth Surface Processes and Landforms*, 32, 1293-1307.

Sancho-García, A., Guillén, J., Ojeda, E. and Piccardo, D. 2008. Inundación de las playas de Barcelona durante temporales. *Geo-Temas*, 10 (2), 583-586.

Stockdon, H.F, Holman, R.A., Howd, P.A. and Sallernger Jr, A.H. 2006. Parameterization of setup, swash and runup. *Coastal Engineering*, 53, 573-588.

Wolf, J. and Flather, R.A. 2005. Modelling waves and surges during the 1953 storm. *Philosophical Transactions of the Royal Society A-Mathematical, Physical and Engineering Sciences*, 363 (1831), 1359 -1375.

ACKNOLEDGEMENT

This work was partially carried out while the first author visited the Department of Physical Geography, Utrecht University, funded by CSIC through a JAE-predoc grant.

Table 2. - Values of the intertidal and supratidal beach slope for each storm event. Accuracy of the theoretical waterline only; in brackets, the number of waterlines used in the linear regression. Accuracy of the inundation parameter.

Event	Beach slope				Observed inundation vs. Inundation parameter					
	β_{int}	β_{sup}	Regression (nº waterlines)		$HoLo^{0.5} + \eta_{surge}$		η_{surge}		$HoLo^{0.5}$	
			R^2	rmse (m)	R^2	rmse (m)	R^2	rmse (m)	R^2	rmse (m)
1	0.022	0.047	0.83 (21)	11.03	0.90	5.97	0.54	13.15	0.39	14.86
2	0.019	0.040	0.91 (87)	8.77	0.87	9.56	0.90	8.32	0.39	20.39
3	0.019	0.040	0.91 (87)	8.77	0.91	8.84	0.92	8.67	0.39	23.43
4	0.015	0.039	0.91 (97)	11.20	0.65	12.36	0.58	13.47	0.24	18.18
5	0.016	0.041	0.93 (126)	11.11	0.86	9.53	0.84	10.44	0.35	20.83
6	0.016	0.044	0.94 (83)	9.43	0.67	14.29	0.39	19.23	0.45	18.32
7	0.016	0.046	0.95 (69)	8.14	0.69	17.88	0.79	14.96	0.14	30.06